

Copper-Azide-Thioarylazoimidazoles – Structure, Spectra, Redox Properties, Magnetism and Theoretical Interpretation

Prasenjit Bhunia,^[a] Debasis Banerjee,^[a] Papia Datta,^[a] Pallepogu. Raghavaiah,^[b] Alexandra M. Z. Slawin,^[c] John D. Woollins,^[c] Joan Ribas,^[d] and Chittaranjan Sinha*^[a]

Keywords: Copper / Bridging ligands / Structure elucidation / Magnetic properties / Redox chemistry

Azido-copper(II) and -copper(I) complexes of 1-alkyl-2-[(*o*-thioalkyl)phenylazo]imidazole (SRaaNR') have been prepared and studied. Complex **2** [Cu(SRaaNR')(μ_{1,1}-N₃)(N₃)₂] dimerises via end-to-end (μ_{1,3})-N₃ to form a tetrameric structure. Azido-copper(I) complexes of the ligands are obtained as MeOH-bridged dimers, [Cu(SRaaNR')(N₃)(μ-OHMe)]₂ (**3**). The electronic spectra suggest that a small reorganisation energy (0.08 eV) is associated with the change in electronic

configuration, structure and oxidation state from Cu^{II} to Cu^I. Redox interconversion, Cu^{II} ↔ Cu^I, [Cu(SMeaaNMe)(μ-N₃)(N₃)₂] (**2a**) ↔ [Cu(SMeaaNMe)(N₃)(μ-OHCH₃)₂] (**3a**), has been performed in one case. The tetranuclear complex shows ferromagnetic and antiferromagnetic interactions. The spectra, redox chemistry and magnetism are explained by DFT studies.

Introduction

Structure and electronic configuration are interrelated properties in transition metal chemistry.^[1–4] The structural change associated with Cu^{II}/Cu^I reorganisation effects is utilised by biochemical systems in copper-containing metalloenzymes.^[4–9] Cu(II)- and Cu(I)-diimine complexes (diimine function, –N=C–C=N–) have attracted much research interest in the field of redox chemistry, photochemistry and photophysics, supramolecular chemistry, bioinorganic and medicinal chemistry, magnetic materials etc., inspiring us to design new ligands isoelectronic to diimine. We have previously reported 2-(arylo)imidazoles^[10–13] with the azoimine (–N=N–C=N–) chelating functional group, which is π-acidic and stabilises low-valent metal oxidation states. 1-Alkyl-2-(arylo)imidazole successfully stabilises the Cu^I state.^[11,12] 1-Alkyl-2-[(*o*-thioalkyl)phenylazo]imidazoles (SRaaNR') are ligands with N(imidazole) (N), N(azo) (N') and S(thioether) donor centres. The reaction of CuCl₂ with SRaaNR' gives a pentacoordinate square pyramidal Cu(SRaaNR')Cl₂ compound.^[13] In this work, we have selected azide (N₃[–]) as counterion, because

of its ability to generate bridging systems with Cu^{II}/Cu^I.^[14–16] Azide may serve as an end-on (μ_{1,1}) and an end-to-end (μ_{1,3}) bridging agent. In general the end-on coordination mode is associated with ferromagnetic coupling, whereas end-to-end bridging leads to antiferromagnetic interactions.^[15] In this work, we report copper(I) complexes of SRaaNR' and ternary complexes of Cu^{II}/Cu^I, SRaaNR' and azide (N₃[–]). The complexes have been characterised by spectroscopic and electrochemical techniques, as well as X-ray diffraction studies. One of the azide-bridging Cu^{II}-SRaaNR' complexes has been used to examine magnetic coupling at variable temperature, and it shows strong ferromagnetic ($J_1 = 13.35 \text{ cm}^{-1}$) and weak antiferromagnetic ($J_2 = -0.55 \text{ cm}^{-1}$) interaction. Redox interconversion has been studied in one case. DFT and TD-DFT computations have been performed on optimised geometries of selected molecules to define electronic structure, spectra, magnetism and redox properties of the complexes both in the gas phase and in solution.

Results and Discussion

1-Alkyl-2-[(*o*-thioalkyl)phenylazo]imidazoles (SRaaNR') have three potential donor centres N(imidazole), N(azo) and S(thioether).^[13] They were synthesised by coupling *o*-(thioalkyl)phenyldiazonium ions with imidazole in aqueous sodium carbonate and purified by solvent extraction and chromatography. The alkylation was carried out by adding alkyl iodide (MeI, EtI) in dry THF solution to the corresponding 2-[(*o*-thioalkyl)phenylazo]imidazole in the presence of sodium hydride.

[a] Inorganic Chemistry Section, Department of Chemistry, Jadavpur University, Kolkata 700032, India
Fax: +91-033-2413-7121
E-mail: c_r_sinha@yahoo.com

[b] Department of Chemistry, Hyderabad Central University, Hyderabad 500046, India

[c] Department of Chemistry, University of St Andrews, St Andrews, Fife KY16 9ST, UK

[d] Departament de Química Inorgànica, Universitat de Barcelona, Diagonal 6487, 08028 Barcelona, Spain

Supporting information for this article is available on the WWW under <http://dx.doi.org/10.1002/ejic.200900648>.

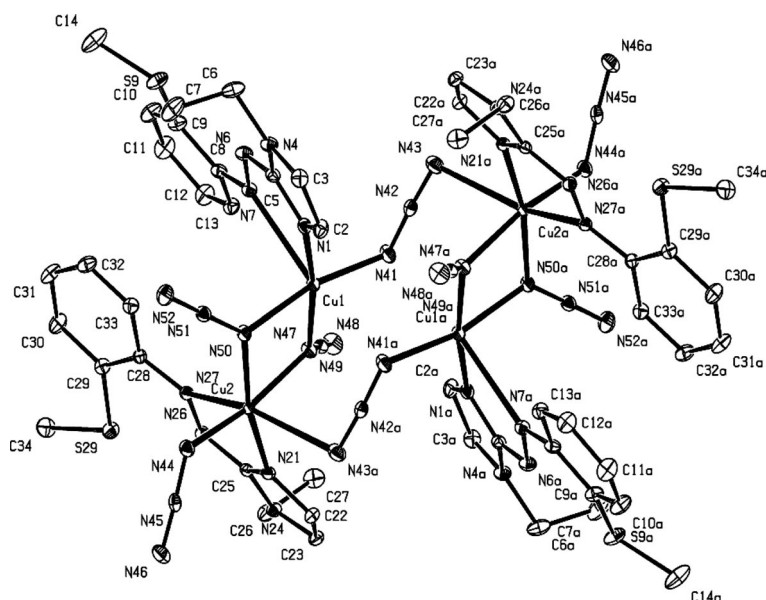
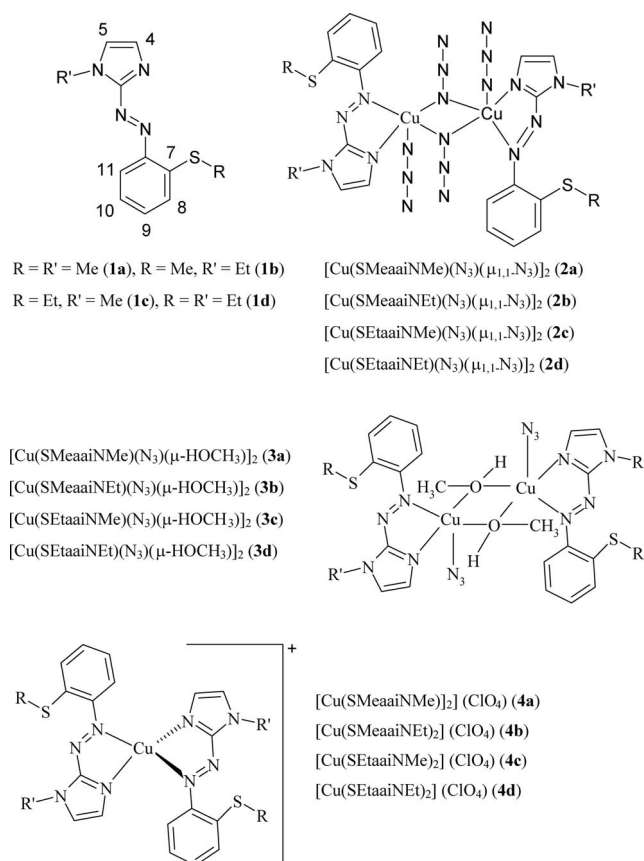


Figure 1. Molecular structure of $[\text{Cu}(\text{SMeaiiNEt})(\mu\text{-N}_3)(\text{N}_3)_2]$ (**2b**) with atom numbering scheme (symmetry codes: $-x + 1$, $-y + 2$, $-z + 1$) (35% ellipsoids shown).

A methanol solution of $\text{Cu}(\text{ClO}_4)_2 \cdot 6\text{H}_2\text{O}$ and the appropriate ligand $\text{SRAaiNR}'$ in a 1:1 mol ratio were treated with aqueous solutions of NaN_3 (2.5 equiv.). Slow evaporation of the solution gave block-shaped brown crystals. The complexes were characterised by microanalytical, spectroscopic, redox and magnetic (bulk and EPR) measurements. The X-ray structure determination in one case shows that **2** has a tetranuclear structure (see the discussion of crystal structure and Figure 1). The complexes are soluble in methanol, ethanol, chloroform, dichloromethane and acetonitrile but insoluble in hydrocarbons (hexane, benzene, toluene). They are nonconducting. Their magnetic moments at room temperature (1.6–1.7 B.M.) are lower than those for typical $S = \frac{1}{2}$ (Cu^{II}) compounds.

The Cu^{I} complexes (Scheme 1) were synthesised by adding $\text{SRAaiNR}'$ (**1**) to a well-stirred solution of NaN_3 and $[\text{Cu}(\text{MeCN})_4](\text{ClO}_4)$ in methanol under dry nitrogen. Brown crystalline compounds separated on slow evaporation of the solvent. The complexes were characterised by C, H, N analyses and spectroscopic data as $[\text{Cu}(\text{SRAaiNR}')(\text{N}_3)(\mu\text{-OHCH}_3)_2]$ (**3**). Structural confirmation has been carried out in one case by single-crystal X-ray crystallography. $[\text{Cu}(\text{SRAaiNR}')_2](\text{ClO}_4)$ (**4**) were synthesised by refluxing mixtures of $[\text{Cu}(\text{MeCN})_4](\text{ClO}_4)$ and $\text{SRAaiNR}'$ in dry MeOH under dry nitrogen. The complexes are fairly soluble in CH_3CN , CHCl_3 , CH_2Cl_2 and are insoluble in hydrocarbons. The molar conductance measurement shows that complexes **2** and **3** are nonconducting and **4** exhibits 1:1 electrolytic conductivity.

The X-ray structure (Figure 1) reveals that complex **2b** has a neutral tetranuclear copper(II) centre comprising a dimer of dinuclear copper(II) subunits. Selected bond lengths and angles are given in Table 1. The ligand, SMeaiiNEt , is a bidentate N(imidazole) (N), N(azo) (N') chelator; $-\text{S}-\text{Me}$ (thioether) remains free and away from the



Scheme 1.

metal centre. There are two crystallographically unique copper(II) environments: one of them is square-based pyramidal CuN_5 , and the second is a distorted octahedral CuN_6 -type environment. The two unique copper atoms are linked

by two $\mu_{1,1}$ -azides, whilst dimerisation of the dinuclear motif is accomplished through $\mu_{1,3}$ -N₃ groups. There are two different N-donor centres of SMeaiiNEt: N(imidazole) [N1, N21 or N1a, N21a] and N(azo) [N7, N27 or N7a, N27a]. The Cu–N distances of these two types of N centres differ significantly by approximately 0.07 Å {Cu–N(azo) [Cu1–N7, 2.6277(16); Cu2–N27, 2.5837(18) Å] and Cu–N(imidazole) [Cu1–N1, 1.9610(16); Cu2–N21, 1.9788(16) Å]}. The stronger binding of N(imidazole) to Cu^{II} may be due to the comparable hardness of Cu^{II} and N(imidazole). This is also observed in copper-containing biomolecules.^[17] The N=N distance [N6–N7/N26–N27] is 1.278(2) Å, which is slightly elongated relative to the free ligand value,^[18] implies some degree of charge delocalisation, d(Cu)→ π^* (azo).^[11–13]

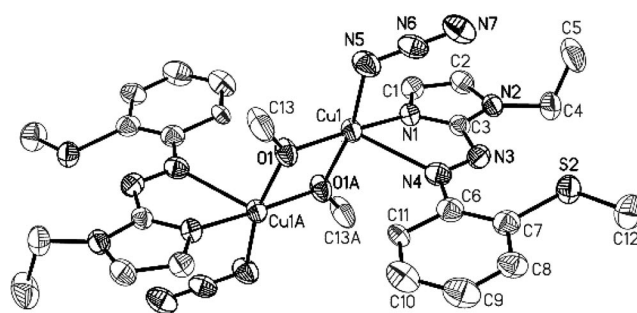
Table 1. Bond lengths and bond angles of **2b** and **3b**.

2b			
Bond lengths / Å		Bond angles / °	
Cu1–N1	1.9610(16)	N1–Cu1–N41	98.02(7)
Cu1–N41	1.9633(17)	N1–Cu1–N47	169.52(7)
Cu1–N47	1.9936(16)	N41–Cu1–N47	92.43(7)
Cu1–N50	2.0120(17)	N1–Cu1–N50	91.89(7)
Cu1–N7	2.628(4)	N41–Cu1–N50	167.41(7)
Cu2–N44	1.9536(17)	N47–Cu1–N50	77.65(7)
Cu2–N21	1.9788(16)	N44–Cu2–N21	100.98(7)
Cu2–N50	1.9987(16)	N44–Cu2–N50	91.17(7)
Cu2–N47	2.0392(17)	N21–Cu2–N50	167.57(7)
Cu2–N27	2.584(3)	N44–Cu2–N47	168.04(7)
N6–N7	1.278(2)	N21–Cu2–N47	90.97(6)
N26–N27	1.278(2)	N50–Cu2–N47	76.91(7)
N41–N42	1.203(2)	N1–Cu1–N7	70.41(6)
N42–N43	1.153(2)	N21–Cu2–N27	70.86(7)
N44–N45	1.205(2)	Cu1–N47–Cu2	101.47(7)
N45–N46	1.158(2)	Cu1–N50–Cu2	102.25(7)
N47–N48	1.215(2)	N43–N42–N41	176.3(2)
N48–N49	1.145(2)	N49–N48–N47	179.1(2)
N50–N51	1.210(2)	Cu1–N50–Cu2	102.25(7)
N51–N52	1.143(2)	Cu1–N47–Cu2	101.47(7)
Cu2a–N43	2.732(3)	N50–Cu1–N47	77.65(7)
Cu1a–N41a	1.963(4)	N50–Cu2–N47	76.91(7)
3b			
Bond lengths / Å		Bond angles / °	
Cu1–N1	1.987(3)	N1–Cu1–N4	71.69(13)
Cu1–N4	2.468(4)	N5–Cu1–N1	93.97(16)
Cu1–N5	1.964(4)	N5–Cu1–N4	89.43(17)
Cu1–O1	1.938(3)	O1–Cu1–O1a*	76.18(13)
Cu1–O1a*	1.939(3)	O1–Cu1–N5	93.40(15)
N3–N4	1.268(5)	O1–Cu1–N5	167.13(16)
N5–N6	1.179(6)	O1–Cu1–N1	171.76(13)
N6–N7	1.156(6)	O1a*–Cu1–N1	96.02(13)
Cu1–Cu1a*	3.0516(11)	O1–Cu1–N4	112.07(13)
		O1–Cu1–N4	101.41(13)
		O1a*–Cu1–Cu1	38.10(8)
		O1a*–Cu1a*–Cu1	38.08(8)
		N7–N6–N5	177.5(5)
		Cu1–O1–Cu1a*	103.82(13)

*Symmetry: $-x + 1, -y + 2, -z + 1$

The single-crystal X-ray structure of [Cu(SMeaiiNEt)(N₃)(μ -OHCH₃)₂] (**3b**) is shown in Figure 2. Selected bond lengths and angles are given in Table 1. The copper(I) centre exhibits a distorted tetrahedral CuN₃O coordination sphere bridged by OHCH₃ and two N centres from chelat-

ing ligand. The ligand, SMeaiiNEt, has three eligible donor centres: N(imidazole), N(azo) and S(thioether); in this case, it acts as an N(imidazole), N(azo) bidentate chelating agent. The chelate angle [Cu–N=N–C=N (N–N)] is 71.69(3)°, which is comparable to the reported data.^[11,12] The deviation of the angle from the ideal 90° for a regular structure is a result of steric requirements of the chelated ligands. The Cu–N(azo) bond length [Cu1–N4, 2.468(4) Å] is longer than the Cu–N(imidazole) distance [Cu1–N1, 1.987(3) Å]. The N=N bond length [N3–N4, 1.268(4) Å] is greater than that of the free ligand value [1.252(1) Å]^[18] but is shorter than that in the Cu^{II} analogue (Table 1, Figure 1), perhaps as a consequence of better $d\pi(\text{Cu}) \rightarrow \pi^*(\text{azo})$ charge overlap^[12,19,20] in this compound than in **2b**. CH₃OH acts as bridging molecule through the O centre, and thus a dimer is formed. The Cu1–O1 distance is 1.939(3) Å. The Cu1...Cu1a distance is too long (3.052 Å) to consider any metal–metal interaction. In the dinuclear motif, the bridging unit Cu₂O₂ is a distorted four-armed plane of mean deviation of approximately 0.02 Å. The bridge angle is Cu1–O1–Cu1a, 103.82(13)° and the remaining angle is O1–Cu1–O1a, 76.18(13)°. The chelate and bridge planes are inclined at an angle of 78.39(16)°.

Figure 2. Thermal ellipsoidal plot with atom labelling scheme of [Cu(SMeaiiNEt)(N₃)(μ -OHCH₃)₂] (**3b**) (30% probability). Atoms with label A are generated by symmetry.

Infrared spectra of complexes **2** exhibit $\nu(\text{N}=\text{N})$ and $\nu(\text{C}=\text{N})$ at 1410–1430 and 1580–1595 cm⁻¹, respectively, and these values are redshifted by 10–25 cm⁻¹ relative to those of the free ligands. This supports coordination of N(azo) and N(imine) to Cu^{II}. The most significant observation is the appearance of a strong doublet at 2090–2105 and 2065–2085 cm⁻¹. These correspond to bridging $\nu_{\text{asym}}(\text{N}_3)$.^[15,16,21]

In complexes **3**, $\nu(\text{N}_3)$ appears as a single sharp stretch at 2035–2045 cm⁻¹. The $\nu(\text{N}=\text{N})$ and $\nu(\text{C}=\text{N})$ appear at 1410–1415 and 1580–1590 cm⁻¹, respectively. The stretching frequency of N=N in [Cu(SRaaNR')(N₃)(μ -OHCH₃)₂] (**3**) appears at a lower value than that for Cu^{II} complexes, [Cu(SRaaNR')(μ -N₃)(N₃)₂] (**2**) ($\Delta\nu = 5$ –10 cm⁻¹), and this effect has been attributed to better $d\pi(\text{Cu}) \rightarrow \pi^*(\text{azo})$ back bonding in copper(I) complexes^[11–13,19] than in copper(II) complexes (also supported by N=N bond length data, vide supra). In [Cu(SRaaNR')₂](ClO₄) (**4**), $\nu(\text{N}=\text{N})$ and $\nu(\text{C}=\text{N})$ appear at 1390–1400 and 1560–1575 cm⁻¹, respec-

Table 2. FTIR^[a] and UV/Vis spectra^[b] of the complexes in CH₃CN.

Compound	UV/Vis spectra λ_{\max} /nm ($10^{-3} \times \epsilon$ /dm ³ mol ⁻¹ cm ⁻¹)	IR spectra /cm ⁻¹			
		$\nu(\text{N}_3^-)$	$\nu(\text{ClO}_4^-)$	$\nu(\text{C}=\text{N})$	$\nu(\text{N}=\text{N})$
2a	725(0.37), 410(27.01), 362(38.11), 265(11.03)	2092, 2065		1581	1423
2b	759(0.12), 413(9.57), 367(13.73), 269(9.31)	2102, 2071		1587	1420
2c	728(0.15), 416(18.31), 364(21.05), 263(9.23)	2090, 2068		1585	1426
2d	726(0.48), 403(20.10), 367(26.34), 268(14.12)	2098, 2069		1590	1443
3a	711(0.18), 434(13.96), 369(13.59), 251(8.41)	2040		1589	1421
3b	715(0.16), 428(12.24), 368(13.27), 259(8.77)	2035		1586	1429
3c	737(0.18), 436(10.45), 371(12.71), 254(7.93)	2043		1590	1455
3d	735(0.18), 434(13.57), 373(12.71), 253(8.19)	2040		1576	1446
4a	762(0.45), 415 (16.54), 359(22.19), 262(15.74)		1094	1591	1429
4b	756(0.41), 410 (14.66), 358(21.47), 260(14.52)		1089	1587	1428
4c	752(0.47), 419 (14.14), 362(21.30), 260(14.15)		1089	1585	1423
4d	765(0.38), 419 (20.11), 352(26.24), 257(15.13)		1090	1590	1428

[a] In KBr disk. [b] In MeCN solution.

tively. The $\nu(\text{ClO}_4)$ frequency appears as a high intense sharp band at 1085–1090 cm⁻¹ with a weak signal at 625 cm⁻¹. Some interesting IR data are given in Table 2.

The electronic spectra of **2** exhibit multiple highly intense transitions ($\epsilon \approx 10^4 \text{ M}^{-1} \text{ cm}^{-1}$) in the visible region, 400–445 nm, along with a broad weak band at 725–760 nm. In the free ligand SRaaiNR', the intraligand charge transitions, $n-\pi^*$ and $\pi-\pi^*$, appear at 370–380 and 250–260 nm, respectively. Some of the transitions are new (Table 2, Figure 3) in the complexes: these are characteristic of copper(II) azoheterocycles^[16,19,22] and are the MLCT transitions involving $d\pi(\text{Cu}) \rightarrow \pi^*(\text{arylazoheterocycle})$. By comparing them with values for copper(II)-1-alkyl-2-(arylamino)imidazoles,^[11–13,16] copper(II)-2-(arylamino)pyridine,^[19] copper(II)-pyridylthioazophenolates^[22] and other pyridylthioethers,^[23] we can assign the transitions at approximately 410 nm to the MLCT [$d\pi(\text{Cu}) \rightarrow \pi^*(\text{azoimidazole})$] band, and the absorption at approximately 740 nm is undoubtedly a d–d transition.^[24] The visible ranges of the spectra of copper(I) complexes (**3**, **4**) show similar metal-to-ligand charge-transfer (MLCT) transitions at 710–765 nm and 410–

435 nm (Figure 3), which are characteristic features of Cu^I complexes when bonded with conjugated organic chromophores.^[14–16]

EPR Spectra

Solid state EPR spectra of **2** at room temperature (298 K) are weakly resolved. Copper(I) complexes **3** and **4** are EPR silent. The hyperfine splitting in the EPR spectra of **2** is poor. The resolution is better at 77 K in MeCN solution (Figure 4). The complexes show the expected four-line (⁶³Cu, $I = 3/2$) EPR spectra and are anisotropic at higher magnetic field, exhibiting axial spectra having g_{\parallel} values varying from 2.188 to 2.226 and A_{\parallel} in a range from 140×10^{-4} to $165 \times 10^{-4} \text{ cm}^{-1}$. The results are in general agreement with the electronic spectra, which also suggest the existence of distorted geometry. From the observed g -tensor values of the Cu^{II} complexes, it is clear that $g_{\parallel} > g_{\perp} > 2.0023$, which agrees with the ground state configuration of $d_{x^2-y^2}$, giving ²B_{1g}.

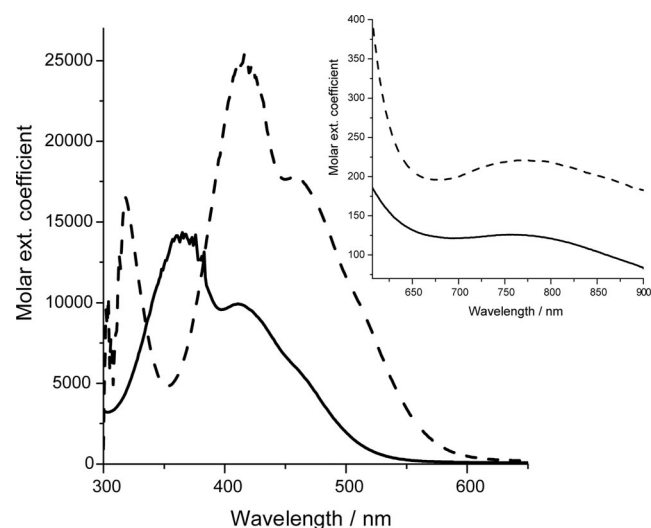


Figure 3. UV/Vis spectra of **2b** (—) and **3b** (---) in DMF at 298 K.

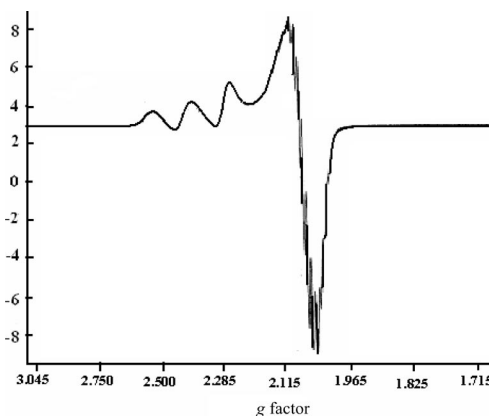


Figure 4. EPR spectrum of [Cu(SEtaaiNEt)(μ-N₃)(N₃)₂] (**2d**) in MeCN at 77 K.

The stereochemistry of [Cu(SRaaiNR')(N₃)(μ-OH-CH₃)₂] (**3**) and [Cu(SRaaiNR')₂](ClO₄) (**4**) was studied by ¹H NMR spectroscopy. The aromatic and imidazole protons are shifted downfield on coordination of SRaaiNR' to

Table 3. ^1H NMR spectroscopic data of $[\text{Cu}(\text{SRaaiNR}')_2](\text{ClO}_4)$ (**4**) and $[\text{Cu}(\text{SRaaiNR}')(\text{N}_3)(\mu\text{-OH CH}_3)]_2$ (**3a**) in CDCl_3 at room temperature.

Compound	δ /ppm (J /Hz)		8H ^d	9, 10-H ^m	11-H ^d	N1-CH ₃ ^s	N1-CH ₂ ^q	N1-CH ₂ CH ₃ ^t	S-CH ₃ ^s	S-CH ₂ ^q	S-(CH ₂)CH ₃ ^t
	4-H ^{b(a)}	5-H ^b									
3a	7.34	7.22	7.45 (7.0)	7.57	7.84 (7.5)	4.28			2.72		
3b	7.38	7.24	7.50 (7.0)	7.55	7.87 (7.5)		4.48 (9.0)	1.68 (8.0)	2.68		
3c	7.36	7.20	7.40 (7.0)	7.60	7.85 (7.5)	4.31				3.36 (7.5)	1.52 (8.0)
3d	7.30	7.30	7.45 (7.0)	7.56	7.88 (7.5)		4.40 (9.0)	1.62 (8.0)		3.40 (7.5)	1.57 (8.0)
4a	7.28	7.27	7.44 (7.0)	7.53	7.86 (8.0)	4.22			2.70		
4b	7.27	7.24	7.46 (7.5)	7.53	7.84 (8.0)		4.74 (9.0)	1.78 (8.0)	2.72		
4c	7.31	7.25	7.43 (7.5)	7.54	7.89 (7.5)	4.24				3.42 (9.0)	1.56 (8.0)
4d	7.30	7.28	7.47 (7.5)	7.56	7.83 (7.5)		4.72 (9.0)	1.75 (8.0)		3.40 (9.0)	1.57 (8.0)

[a] ^b Broad singlet; ^d doublet; ^m multiplet; ^s singlet; ^t triplet; ^q quartet.

Cu^{I} relative to the free ligand data^[11,12] (Table 3). This implies significant bonding interaction of the metal ion with the ligand. Imidazole protons (4- and 5-H) and aryl protons (8–11-H) suffer approximately 0.10 to 0.15 ppm downfield shift. The S–R and N1–R' do not shift significantly, which implies a non-coordinated –S–R centre. Ligands SRaaiNR' are capable of showing a tridentate N,N',S donor system. However, ^1H NMR spectroscopic data reflect no coordination of –S–R to Cu^{I} , thus these ligands serve as bidentate N,N' chelators.

The magnetic properties of complex **2b** are shown in Figure 5 as a $\chi_{\text{M}}T$ vs. T plot (χ_{M} is the molar magnetic susceptibility for two Cu^{II} ions). The value of $\chi_{\text{M}}T$ at 300 K is $0.86 \text{ cm}^3 \text{ mol}^{-1} \text{ K}$, a typical value for two copper(II) ions with $g > 2.00$, as expected. On lowering the temperature, there is a rapid increase in $\chi_{\text{M}}T$ to $1.03 \text{ cm}^3 \text{ mol}^{-1} \text{ K}$ at 5 K and then a decrease to $0.91 \text{ cm}^3 \text{ mol}^{-1} \text{ K}$ at 2 K. These features indicate noticeable intramolecular ferromagnetic coupling with the presence of weak intermolecular antiferromagnetic interactions, always present at very low temperature.

The plot of the reduced magnetisation at 2 K is included in Figure 5. The $M/N \mu_{\text{B}}$ value at saturation (5 T) is 2.00, in agreement with the presence of two electrons in the ground state.

Complex **2b** is a tetranuclear entity, constituted by dimerisation of two Cu_2 “dinuclear entities”. In the “dinuclear entity” each Cu^{II} is linked by two azido ligands in an end-on ($\mu_{1,1}\text{-N}_3$) coordination mode. Furthermore, one of the terminal azido ligands of each dinuclear unit links the neighbouring dinuclear entity by means a long apical Cu–N(azido) bond. (Figure 1). The resulting tetranuclear entity, together with the two different magnetic pathways (J_1 and J_2) are depicted in Scheme 2.

For calculating the values of J_1 and J_2 two approaches have been carried out. First, we have considered the Cu_2 “dinuclear entity” by applying the Bleaney–Bowers formula,^[25] with the Hamiltonian $H = -J_1 \sum S_i S_j$, and introduc-

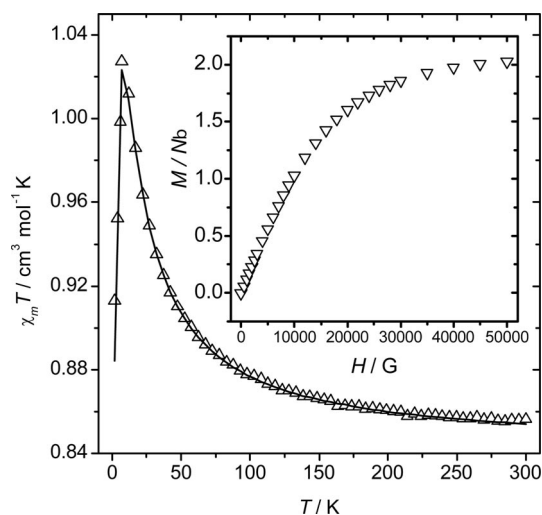
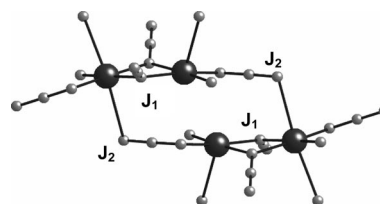


Figure 5. Plot of the susceptibility data, $\chi_{\text{M}}T$ vs. T , for **2b**, assuming a dinuclear entity. The solid line represents the best fit using the J_2 parameter with the mean field approach (see text for explanation). Inset: plot of the reduced magnetisation $M/N \mu_{\text{B}}$ vs. H data at 2 K.



Scheme 2.

ing a J_2 parameter through the mean-field approach for calculating the intermolecular interactions.^[26,27] This approach is valid because of the long apical Cu–N(azido) distance, which allows to assume a very weak magnetic coupling. The best-fit parameters were: $J_1 = 13.35 \pm 0.5 \text{ cm}^{-1}$, $g =$

2.12 ± 0.002 , $J_2 = -0.55 \pm 0.01 \text{ cm}^{-1}$ and $R = 4.0 \times 10^{-5}$ $\{R$ is the agreement factor defined as $\sum_i [(\chi_m T)_{\text{obs}} - (\chi_m T)_{\text{calc}}]^2 / \sum_i [(\chi_m T)_{\text{obs}}]^2$.

The second approach consists of considering the tetranuclear complex as an isolated entity. The corresponding fit can be made by applying the corresponding formula for the model indicated in Scheme 2 or, more easily, by working with the Clumag program,^[28] using the same Hamiltonian and with the coupling values shown in Scheme 2. Both models are exact, and thus the results are identical and independent of the method. The best-fit parameters are: $J_1 = 11.25 \pm 0.5 \text{ cm}^{-1}$, $J_2 = -0.85 \pm 0.02 \text{ cm}^{-1}$, $g = 2.12 \pm 0.01$ and $R = 3.7 \times 10^{-3}$ $\{R$ is the agreement factor defined as $\sum_i [(\chi_m T)_{\text{obs}} - (\chi_m T)_{\text{calc}}]^2 / \sum_i [(\chi_m T)_{\text{obs}}]^2$.

By applying two different methods, we have obtained very similar results, as expected: J_1 is medium and positive (ferromagnetic) and J_2 is weak and negative (antiferromagnetic).

All experimentally reported complexes,^[29] as well as theoretical studies,^[30] have demonstrated that almost all dinuclear complexes with double azido ligand bridges in the $\mu_{1,1}$ coordination mode create ferromagnetic coupling. All data seem to indicate that the main parameter is the M–N–M angle (N referring to the N_3 bridging ligand). For Cu^{II} , when this angle is extraordinarily large, for example greater than 108° , the magnetic coupling becomes antiferromagnetic.^[31] In fact, almost all complexes have a Cu–N–Cu angle between 96° and 104° , thus being ferromagnetic. Many other structural factors may influence the J value, such as the Cu–N distance and the Cu–N₃–Cu torsion angle.^[32] A clear dependence of the exchange coupling constant on the Cu–N distance has been found, the ferromagnetic coupling decreasing as the Cu–N distance increases.^[30] The J_1 value found for complex **2b** is rather small compared to those reported in the literature.^[30] The three most important factors are: the Cu–N–Cu angles [Cu1–N50–Cu2 $102.25(7)^\circ$ and Cu1–N47–Cu2 $101.47(7)^\circ$], the Cu–N distances (these are rather long, from 1.994 to 2.039 Å) and the τ torsion angles (these are very large). The sum of these factors causes the relatively small J_1 parameter. Assuming a tetranuclear entity, the J_2 value (-0.85 cm^{-1}) is easily understood by taking into account the long Cu(apical)–N(azido) distance (2.73 Å).

Copper(I) complexes $[\text{Cu}(\text{SRAaiNR}')(\text{N}_3)(\mu\text{-OHCH}_3)_2]$ (**3**) show oxidative responses at approximately 0.4 V. This is quasireversible, as estimated from peak-to-peak separation ($\Delta E_p > 100 \text{ mV}$) and is assigned to the $\text{Cu}^{\text{II}}/\text{Cu}^{\text{I}}$ couple by comparison with literature reports.^[11,12,19] Complexes $[\text{Cu}(\text{SRAaiNR}')_2](\text{ClO}_4)$ (**4**) show a higher $\text{Cu}^{\text{II}}/\text{Cu}^{\text{I}}$ potential, which may be due to the presence of two π -acid-coordinated azoimine functions. Figure 6 shows the cyclic voltammogram (CV) of the complexes in MeOH (Table 4). The CV plots of copper(II) complexes **2** show a reductive response at approximately 0.4 V vs. SCE. On comparing with the CV of $\text{Cu}(\text{RaaiR}')_2\text{X}_2$ ($\text{X} = \text{N}_3, \text{NCS}$),^[10] the couple is assigned to a $\text{Cu}^{\text{II}}/\text{Cu}^{\text{I}}$ couple. On scanning in the negative direction up to -1.8 V , we observe an irreversible response, E_{pc} , at approximately -0.4 V and a quasireversible one at

-1.0 to -1.2 V ($\Delta E_p > 140 \text{ mV}$) (Figure 6), which may be assigned to reduction of the azo groups $[(-\text{N}=\text{N}-)/(-\text{N}=\text{N}-)]$ of the chelated ligands. The free ligand does not show any oxidation, but irreversible reductive responses appear at $< -1.0 \text{ V}$. The voltammogram also shows a sharp anodic part at approximately -0.2 V , possibly due to the $\text{Cu}^{\text{I}}/\text{Cu}^0$ couple.^[12,33] The reduced Cu^0 is absorbed on the electrode surface, as evidenced by the narrow width of the anodic response with a large peak current.

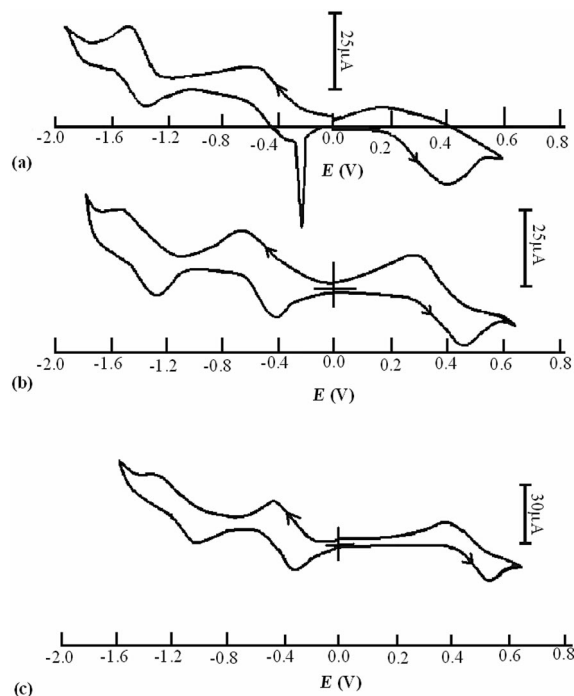


Figure 6. Cyclic voltammogram of (a) **2a**, (b) **3a** and (c) **4a** in CH_2Cl_2 .

Table 4. Cyclic voltammetric data.^[a]

Complex	Metal redox couple		Ligand redox couple	
	E/V ($\Delta E_p/\text{mV}$) $\text{Cu}^{\text{II}}/\text{Cu}^{\text{I}}$	$\text{Cu}^{\text{I}}/\text{Cu}^0$	E/V ($\Delta E_p/\text{mV}$) azo/azo ⁻	azo ⁼ /azo ⁻
2a	0.33 (150)	-0.25 ^[b]	-0.48 (160)	-1.40 (170)
2b	0.37 (170)	-0.22 ^[b]	-0.44 (180)	-1.35 (200)
2c	0.38 (160)	-0.22 ^[b]	-0.44 (160)	-1.30 (200)
2d	0.40 (140)	-0.24 ^[b]	-0.48 (180)	-1.38 (180)
3a	0.37 (120)		-0.58 (150)	-1.42 (170)
3b	0.35 (128)		-0.54 (170)	-1.38 (200)
3c	0.30 (130)		-0.56 (180)	-1.42 (200)
3d	0.38 (140)		-0.58 (160)	-1.38 (180)
4a	0.44 (180)		-0.40 (140)	-1.22 (190)
4b	0.42 (180)		-0.47 (160)	-1.24 (200)
4c	0.40 (180)		-0.44 (170)	-1.27 (200)
4d	0.44 (110)		-0.44 (160)	-1.24 (140)

[a] Solvent: MeCN; Pt-disk working electrode, supporting electrolyte: TBAP (0.01 M); reference: SCE; solute concentration: 10^{-3} M ; scan rate: 0.05 V s^{-1} ; $\Delta E_p = |E_{\text{pa}} - E_{\text{pc}}| \text{ mV}$; E_{pa} = anodic peak potential, E_{pc} = cathodic peak potential in V; $E_{1/2} = 0.5(E_{\text{pa}} + E_{\text{pc}}) \text{ V}$. [b] E_{pc} .

DFT calculation has been performed for two different molecules, **2b** and **3b**. The optimised structure of these molecules are developed by using the Gaussian 03 analysis

package. The orbital energies along with contributions from the ligands and metal are given in the Supporting Information. Figure 7 depicts selected occupied and unoccupied frontier orbitals. In Cu^{II} complex **2b**, the highest occupied molecular orbital (MO) is singly occupied, so it is abbreviated as SOMO. The occupied MOs are stabilised, whereas unoccupied MOs are destabilised on going from the Cu^{II} (**2b**) to the Cu^I (**3b**) compounds: $E_{\text{SOMO}}(\mathbf{2b}) = -4.9$ eV and $E_{\text{HOMO}}(\mathbf{3b}) = -4.17$ eV. This may be due to better electron donation from Cu^I (d¹⁰) compared to that from Cu^{II} (d⁹) toward the π -acidic azoimine function. Solvent polarity stabilises occupied MOs more efficiently than unoccupied MOs. Thus, the energy separation (ΔE) between the SOMO (for **2b**) or HOMO (for **3b**) and the LUMO increases on going from the gas phase to the MeCN phase. The occupied MOs (HOMO-1 and HOMO-2) of **2b** have a significant contribution from Cu (ca. 10%). The bridging azide ($\mu_{1,1}$ and $\mu_{1,3}$ -N₃) contributes 7% to the HOMO, while the terminal azide contributes 89%. In complex **3b** copper contributes 42% to the HOMO and 13% to the LUMO. Azide contributes to the HOMO

(ca. 39%). The chelating ligand SMeaaiNET, in general, is the main constituent of unoccupied MOs (**2b**: LUMO to LUMO+10, 99–100% and **3b**: LUMO, 73%; LUMO+1, 95%). The charge-transfer transition in the visible region not observed in the free ligand is assigned to pure MLCT rather than an admixture of $d\pi(\text{Cu}) \rightarrow \pi^*(\text{azoimine})$ and $\pi(\text{azide}) \rightarrow \pi^*(\text{azoimine})$ transitions involving the SOMO \rightarrow LUMO/LUMO+1/LUMO+2 and HOMO-1/HOMO-2/HOMO-3 \rightarrow LUMO/LUMO+1//LUMO+2 functions. The ILCT $\pi(\text{thioazoimidazole}) \rightarrow \pi^*(\text{azoimine})$ transitions may appear in the high energy region. In Cu^I complex **3b**, the transitions HOMO/HOMO-1/HOMO-3 \rightarrow LUMO/LUMO+1/LUMO+2 have significant $d\pi(\text{Cu}) \rightarrow \pi^*(\text{thioazoimidazole})$ contribution.

Cyclic voltammetric behaviour of **3** and **4** are readily rationalised by using the DFT calculation. Because of higher metal (Cu) function in occupied MOs in **3b**, the complexes show metal oxidation. Unoccupied MOs are significantly dominated by the azoimine function, thus reduction may refer to electron addition at the azo-dominated orbital of the ligand.

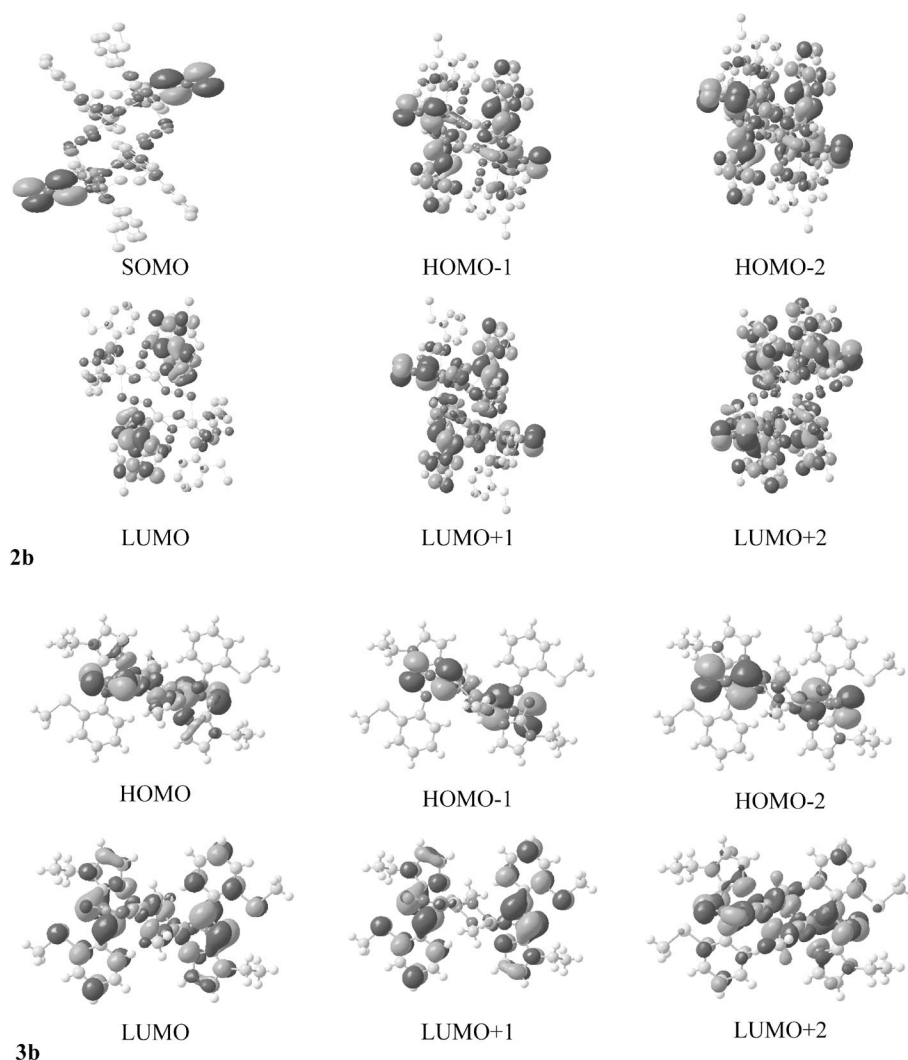
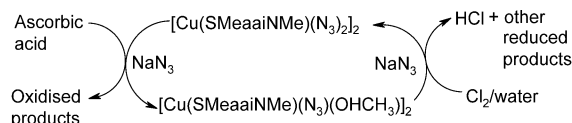


Figure 7. Selected molecular orbital pictures of **2b** and **3b**.

The spin density calculated for the triplet state from a DFT study determines the exchange coupling between the two metal centres. The degree of delocalisation of the unpaired electron increases if the coordinating atoms of the ligand participate in the singly occupied molecular orbital (SOMO), which leads to the enhancement of the electron density of the donor atoms. Interestingly, the spin density is mainly distributed among the copper $d_{x^2-y^2}$ magnetic orbital and $\mu_{1,1}$ - N_3 bridging between two Cu centres $[Cu^I \cdots Cu^I]$ in the dinuclear entity. It is to be noted that the exchange coupling constant for **2b** calculated by using the crystal coordinates suggests a ferromagnetic interaction (J) of 10.76 cm^{-1} . For the optimised geometry, the calculated (UB3LYP) average Cu- μ -N($\mu_{1,1}$ - N_3) bond length is 1.98 \AA , which is comparable with the average X-ray value (2.03 \AA). The other bond lengths within the coordination sphere deviate marginally from the experimentally observed values. In terms of magnetic properties, the Cu^I- μ -N($\mu_{1,1}$ - N_3)-Cu^I angle is the most important. According to the Hay model,^[33] the antiferromagnetic exchange coupling constant for the binuclear metal complexes, each bearing one unpaired electron, is linearly proportional to the square of the energy difference between the two SOMOs. The overlap between the magnetic orbitals of the copper atoms takes place via the bonding between the $d_{x^2-y^2}$ magnetic orbital of copper and the hybrid orbital of the bridging azido-N. Thus, the spin delocalisation on the bridging group corroborates the antiferromagnetic interaction.

Redox Interconversion Cu^{II} \leftrightarrow Cu^I

The Cu^{II}-Cu^I interconversion experiment was carried out by using a representative compound of the series, $[Cu(SMeaaiNMe)(\mu-N_3)(N_3)]_2$ (**2a**). Compound **2a** reacts with ascorbic acid in aqueous methanol in the presence of NaN_3 (an excess amount of NaN_3 is added to resist dissociation), and a brown-red copper(I) complex precipitates. The identity of the reduced product has been established by matching the spectroscopic and cyclic voltammetric results (Table 2 and Table 4). The compound is diamagnetic. The structure of the coordinated Cu^I compound was established by its ¹H NMR spectrum and by comparison with the spectrum of directly synthesised $[Cu(SMeaaiNMe)(N_3)(\mu-OHCH_3)]_2$ (**3a**) (Table 3). Microanalytical data (C,H,N) also confirm the composition of the compound. In a second experiment, to a suspension of $[Cu(SMeaaiNMe)(N_3)(\mu-OHCH_3)]_2$ (**3a**) in methanol was added chlorine water, and the mixture was stirred in air. Nitrogen gas was bubbled through the solution to remove chlorine followed by the addition of excess NaN_3 , whereupon the colour of the solution changed to brown-red. A crystalline compound was precipitated by reducing the volume of the solution to half. The compound so obtained was purified by crystallisation from $CH_2Cl_2/MeOH$. The spectroscopic (IR and UV/Vis), magnetic and voltammetric identification support the formation of copper(II) complex **2a**, which is supported by microanalytical data and spectral measurements.



Conclusion

1-Alkyl-2-[(*o*-thioalkyl)phenylazo](SRaaiNR') coordinates to Cu^{II} and Cu^I in the presence of azide (N_3^-) as a bidentate N,N' -chelator. Tetranuclear Cu^{II}-azido-bridged complexes show ferromagnetic and antiferromagnetic coupling. Electrochemistry shows a quasireversible Cu^{II}/Cu^I redox couple along with Cu^I/Cu⁰ response at -0.2 V . The solution spectra show highly intense metal-to-azoimine charge transfer. Cu^{II} (**2**) and Cu^I (**3**) complexes undergo redox interconversion; Cu^{II} complex **2b** is reduced by ascorbic acid to a Cu^I complex in methanol in the presence of excess NaN_3 , whilst Cu^I complex **3a** is oxidised by chlorine water to Cu^{II} complex (**2**). The spectra, magnetism and redox properties are explained by using DFT computation on optimised geometries.

Experimental Section

Materials: All starting organic compounds were purchased from Aldrich Chemical Co. and used without further purification. $CuCl_2 \cdot 2H_2O$ and NaN_3 were E. Merck reagent grade. Solvents were distilled from appropriate drying agents under appropriate conditions as per literature in a N_2 atmosphere.^[34] $[Cu(MeCN)_4](ClO_4)$ was used as copper(I) precursor. All experiments were carried out under N_2 . The syntheses of the ligands were carried out by following the common procedure^[13] of coupling the *o*-(thioalkyl)phenyldiazonium ion [obtained by diazotisation of *o*-(thioalkyl)aniline] with imidazole at pH 7 followed by N1-alkylation using alkyl iodide in the presence of NaH in dry THF under dry and inert conditions.

Caution! Perchlorate salts of metal complexes can be explosive. Although no detonation tendencies have been observed, care is advised and handling of only small quantities recommended.

Physical Measurements: Microanalytical data (C,H,N) were collected with a Perkin-Elmer 2400 CHNS/O elemental analyser. Spectroscopic data were obtained by using the following instruments: Perkin-Elmer model Lambda 25 spectrophotometer (UV/Vis), Perkin-Elmer model RX-1 spectrometer on KBr disks at $4000\text{--}450 \text{ cm}^{-1}$ (IR), Bruker (AC) 300 MHz FTNMR spectrometer (¹H NMR). Electrochemical measurements were performed by using computer-controlled PAR model 250 VersaStat electrochemical instruments with Pt disk electrodes. All measurements were carried out under nitrogen at 298 K with reference to SCE in acetonitrile and by using $[nBu_4N][ClO_4]$ as supporting electrolyte. The reported potentials are uncorrected for the junction potential. Room temperature (298 K) magnetic susceptibility was measured with a Sherwood Scientific (Cambridge, UK) instrument at 298 K, and data were corrected by subtracting the diamagnetic contribution. The diamagnetic correction was calculated by individually adding the diamagnetic contribution of each atom using Pascal's constants. EPR spectra were recorded in MeCN solution at room temperature (298 K) and liquid nitrogen temperature (77 K) by using a Bruker model EMX 10/12 ESR spectrometer with an X-band ER 4119 HS cylindrical resonator.

Synthesis of Complexes

Copper(II) Complexes. Preparation of [Cu(SMeaaiNMe)(μ -N₃)(N₃)₂] (2a): 1-Methyl-2-[*o*-(thiomethyl)phenylazo]imidazole (SMeaaiNMe) (200 mg, 0.86 mmol) in methanol (10 mL) was added dropwise to a methanol solution (10 mL) of Cu(ClO₄)₂·6H₂O (330 mg, 0.89 mmol) at 298 K under N₂. The brown-red solution was stirred for 10 min, and a methanol solution of NaN₃ (145 mg, 2.22 mmol) was added. It was then filtered and left undisturbed for a week. Dark brown crystalline compounds were separated. The crystals were filtered, washed with water and cold methanol and dried in vacuo. The yield was 200 mg (61%).

All other complexes were prepared by the same procedure. The yield varied from 60 to 75%. Microanalytical data: found (calcd.) [%] for [Cu(SMeaaiNMe)(μ -N₃)(N₃)₂] (2a), (C₁₁H₁₂N₁₀SCu)₂ (759): C, 34.84 (34.78); H, 3.07 (3.16); N, 36.96 (36.89). [Cu(SMeaaiNMe)(μ -N₃)(N₃)₂] (2b), (C₁₂H₁₄N₁₀SCu)₂ (787): C, 36.55 (36.59); H, 3.47 (3.56); N, 35.65 (35.58). [Cu(SEtaaiNMe)(μ -N₃)(N₃)₂] (2c), (C₁₂H₁₄N₁₀SCu)₂ (787): C, 36.50 (36.59); H, 3.61 (3.56); N, 35.68 (35.58). [Cu(SEtaaiNMe)(μ -N₃)(N₃)₂] (2d), (C₁₃H₁₆N₁₀SCu)₂ (815): C, 38.18 (38.28); H, 3.88 (3.93); N, 34.48 (34.36).

Copper(I) Complexes. Preparation of [Cu(SMeaaiNMe)(N₃)(μ -OHCH₃)₂] (3a): To a dry methanol solution of [Cu(MeCN)₄](ClO₄) (133 mg, 0.40 mmol) was added solid sodium azide (5 equiv., 132 mg, 2.03 mmol) whilst stirring at room temperature in an inert atmosphere (N₂). Then a dry methanol solution of SMeaaiNMe (95 mg, 0.41 mmol) was added by a syringe in an inert atmosphere. The resultant deep brown solution was stirred for one hour and then heated under reflux for another one hour. The solution was filtered, and the filtrate was kept undisturbed for crystallisation. After a few days, deep brown crystals appeared, which were separated by filtration. The crystals were washed with dilute methanol (1:1, v/v) and dried with CaCl₂ in a desiccator. The complexes were characterised by C,H,N analysis, and spectroscopic data support the composition [Cu(SMeaaiNMe)(N₃)(μ -OHCH₃)₂] (3a).

All other complexes were prepared by the same procedure. The yield varied from 65 to 75%. Microanalytical data: found (calcd.) [%] for [Cu(SMeaaiNMe)(N₃)(μ -OHCH₃)₂] (3a), (C₁₂H₁₆N₇OSCu)₂ (739): C, 38.88 (38.97); H, 4.26 (4.33); N, 26.56 (26.52). [Cu(SMeaaiNMe)(N₃)(μ -OHCH₃)₂] (3b), (C₁₃H₁₈N₇OSCu)₂ (767): C, 40.59 (40.68); H, 4.72 (4.69); N, 25.48 (25.55). [Cu(SEtaaiNMe)(N₃)(μ -OHCH₃)₂] (3c), (C₁₃H₁₈N₇OSCu)₂ (767): C, 40.62 (40.68); H, 4.64 (4.69); N, 25.50 (25.55). [Cu(SEtaaiNMe)(N₃)(μ -OHCH₃)₂] (3d), (C₁₄H₂₀N₇OSCu)₂ (795): C, 42.17 (42.26); H, 5.00 (5.03); N, 24.58 (24.65).

Preparation of [Cu(SMeaaiNMe)₂](ClO₄) (4a): The ligand SMeaaiNMe (100 mg, 0.43 mmol) in dry MeOH (25 mL) was added to a methanol solution (20 mL) of [Cu(MeCN)₄](ClO₄) (70 mg, 0.21 mmol) in N₂ at room temperature. The dark-brown solution was stirred for 3 h. The solution was reduced to half of its original volume by bubbling N₂ gas through it, a brown-red crystalline precipitate appeared, which was filtered, washed with methanol/water (1:1, v/v) and dried with CaCl₂. The dried compound was purified by column chromatography. A column alumina (neutral) was prepared in benzene. A chloroform solution of the complex was absorbed in the column and eluted first by chloroform. Initially a light yellow band was eluted and rejected. The desired deep brown/red band was collected by elution by using a methanol/chloroform (4:1, v/v) mixture and concentrated slowly in air. The yield was 0.28 g (52%).

All other complexes were prepared by following identical procedures with yields of 55–70%. Microanalytical data: found (calcd.)

[%] for [Cu(SMeaaiNMe)₂](ClO₄) (4a), (C₂₂H₂₄N₈O₄S₂ClCu) (627): C, 42.04 (42.11); H, 3.88 (3.83); N, 17.92 (17.86). [Cu(SMeaaiNMe)₂](ClO₄) (4b), (C₂₄H₂₈N₈O₄S₂ClCu) (655): C, 43.84 (43.97); H, 4.33 (4.27); N, 17.00 (17.10). [Cu(SEtaaiNMe)₂](ClO₄) (4c), (C₂₄H₂₈N₈O₄S₂ClCu) (655): C, 44.04 (43.97); H, 4.20 (4.27); N, 17.21 (17.10). [Cu(SEtaaiNMe)₂](ClO₄) (4d), (C₂₆H₃₂N₈O₄S₂ClCu) (683): C, 45.63 (45.68); H, 4.75 (4.69); N, 16.32 (16.40).

Copper(II)–Copper(I) Interconversion

[Cu(SMeaaiNMe)(μ -N₃)(N₃)₂] (2a) → [Cu(SMeaaiNMe)(N₃)(μ -OHCH₃)₂] (3a): To a suspension (15 mL) of [Cu(SMeaaiNMe)(μ -N₃)(N₃)₂] (2a) (0.20 g, 0.26 mmol) in methanol was added with stirring under N₂ ascorbic acid (0.09 g, 0.50 mmol) in water (5 mL). The brown suspension quickly changed to deep red-brown, and stirring was continued for 30 min. NaN₃ (0.2 g, excess amount) was added to this solution and stirred. The volume of the solution was reduced by bubbling off N₂ gas, and a precipitate appeared within a short while. The precipitated mass was filtered, washed with water and cold methanol. The residue was dried with CaCl₂ and recrystallised by diffusion of CH₂Cl₂ solution to hexane. Brown shining crystals were isolated. The yield of [Cu(SMeaaiNMe)(N₃)(μ -OHCH₃)₂] (3a) was 0.08 g (42%). Microanalytical data: found (calcd.) [%] for [Cu(SMeaaiNMe)(N₃)(μ -OHCH₃)₂] (3a), (C₁₂H₁₆N₇OSCu)₂ (739): C, 38.92 (38.97); H, 4.36 (4.33); N, 26.45 (26.52).

[Cu(SMeaaiNMe)(N₃)(μ -OHCH₃)₂] (3a) → [Cu(SMeaaiNMe)(μ ,1,1-N₃)(N₃)₂] (2a): To a methanol suspension of [Cu(SMeaaiNMe)(N₃)(μ -OHCH₃)₂] (3a) (0.20 g, 0.27 mmol) methanol saturated with chlorine was added in drops and the mixture was stirred in air. Immediately, the colour changed from red-brown to deep brown. The stirring was continued for 45 min, and then N₂ gas was bubbled for a few minutes with constant stirring. Excess NaN₃ (0.2 g) in water was added, and air was bubbled through the mixture for 30 min and methanol was added from time to time to maintain the volume of the solution at 25 mL. The mixture was filtered and kept in the freezer for 4 h. The brown precipitate was filtered and washed with water and cold methanol. The compound was soluble in the mixture of 2-methoxy ethanol and methanol (1:5, v/v) and was crystallised by concentration in air for a week. The yield of [Cu(SMeaaiNMe)(μ ,1,1-N₃)(N₃)₂] (2a) was 0.12 g (58%). Microanalytical data: found (calcd.) [%] for [Cu(SMeaaiNMe)(μ ,1,1-N₃)(N₃)₂] (2a), (C₁₁H₁₂N₁₀SCu)₂ (759): C, 34.74 (34.78); H, 3.19 (3.16); N, 36.92 (36.89).

X-ray Crystal Structure Analysis of 2b and 3b: Details of crystal analysis, data collection and structure refinement are given in Table 5. Data for 2b (blue colour, prism shape, size 0.20 × 0.20 × 0.05 mm) were collected at 93(2) K by using a Rigaku MM007/Mercury CCD diffractometer (Mo-K α radiation, confocal optics λ = 0.71073 Å). All refinements were performed by using SHELXTL.^[35] Data for 3b (brown colour, plate shape, size 0.36 × 0.18 × 0.10 mm) were collected with a Bruker SMART CCD area detector using fine-focus sealed tube graphite monochromatised Mo-K α radiation (λ = 0.71073 Å) at 293(2) K. Data were corrected for Lorentz polarisation effects and for linear decay. Semiempirical absorption corrections based on ψ -scans were applied. The structure was solved by direct methods using SHELXS-97^[35] and successive difference Fourier syntheses.^[36] All non-hydrogen atoms were refined anisotropically. The hydrogen atoms were fixed geometrically and refined by using the riding model. In the final difference Fourier map, the residual minima and maxima were –0.315 and 0.455 e/Å³ for 2b and –0.400 and 0.647 e/Å³ for 3b. The structures were drawn by using the ORTEP-32^[37] and PLATON-99^[38] programs.

Table 5. Summary of crystallographic data for **2b** and **3b**.

	2b	3b
Empirical formula	C ₂₄ H ₂₈ Cu ₂ N ₂₀ S ₂	C ₂₆ H ₃₄ Cu ₂ N ₁₄ O ₂ S ₂
Formula weight	787.86	765.87
Temperature /K	93(2)	293(2)
Crystal system	monoclinic	monoclinic
Space group	<i>P</i> 2 ₁ / <i>n</i>	<i>P</i> 2 ₁ / <i>c</i>
Crystal size /mm	0.20 × 0.20 × 0.05	0.36 × 0.18 × 0.10
<i>a</i> /Å	14.951(4)	10.8091(19)
<i>b</i> /Å	14.922(3)	13.737(2)
<i>c</i> /Å	15.245(4)	15.4200(19)
β /°	100.474(7)	133.081(7)
<i>V</i> /Å ³	3344.6(14)	1672.3(4)
<i>Z</i>	4	2
μ (Mo- <i>K</i> α) /mm ⁻¹	1.448	1.445
θ range /°	2.22–25.35	2.34–25.36
<i>hkl</i> range	–17 ≤ <i>h</i> ≤ 18; –16 ≤ <i>k</i> ≤ 17; –18 ≤ <i>l</i> ≤ 14	–13 < <i>h</i> < 13; –16 < <i>k</i> < 16; –18 < <i>l</i> < 18
<i>D</i> _{calc} /Mg m ⁻³	1.565	1.521
Refined parameters	436	211
Total reflections	19901	16956
Unique reflections	5971	3259
<i>R</i> ₁ ^[a] [<i>I</i> > 2σ(<i>I</i>)]	0.0286	0.0529
<i>wR</i> ₂ ^[b]	0.0703	0.1607
Goodness of fit	1.025	1.063

[a] $R = \sum |F_o| - |F_c| / \sum |F_o|$. [b] $wR_2 = [\sum w(F_o^2 - F_c^2)^2 / \sum w(F_o^2)^{1/2}]^{1/2}$, $w = 1 / [\sigma^2(F_o^2) + (0.0336P)^2 + (2.7488P)]$ for **2b**; $w = 1 / [\sigma^2(F_o^2) + (0.0942P)^2 + (1.1087P)]$ for **3b** where $P = (F_o^2 + 2F_c^2) / 3$.

CCDC-691681 {[Cu(SMeaiiNEt)(μ-N₃)(N₃)₂] (**2b**)} and -691682 {[Cu(SMeaiiNEt)(N₃)(μ-OHCH₃)₂] (**3b**)} contain the supplementary crystallographic data for this paper. These data can be obtained free of charge from The Cambridge Crystallographic Data Centre via www.ccdc.cam.ac.uk/data_request/cif.

Computational Methods: All computations were performed by using the Gaussian03 (G03)^[39] software package running under Windows. Becke's three-parameter hybrid exchange functional and the Lee–Yang–Parr nonlocal correlation functional^[40] (B3LYP) were used throughout. Elements were assigned a 6-31G* basis set in our calculations. For copper, the Los Alamos effective core potential plus double zeta (LanL2DZ)^[41,42] basis set was employed. Gas- and solution-phase geometry optimisation were carried out from the geometry obtained from the crystal structure without any symmetry constraints. In all cases, vibrational frequencies were calculated to ensure that optimised geometries represented local minima.

Magnetic Measurements: Magnetic measurements were carried out in the “Servei de Magnetoquímica (Universitat de Barcelona)” on polycrystalline samples (30 mg) with a Quantum Design SQUID MPMS-XL magnetometer working in the 2–300 K range. The magnetic field was 0.1 T. Diamagnetic corrections were evaluated from Pascal's constants.

Supporting Information (see also the footnote on the first page of this article): Percentage orbital contribution of **2b** and **3b** in the gas phase, calculated transitions of **3b** with oscillator strength.

Acknowledgments

Financial support from University Grants Commission, New Delhi is thankfully acknowledged. J. R. acknowledges the financial support given by the Spanish Government (Grant CTQ2006-03949).

- [1] A. C. Steenbergen, E. Bouwman, R. A. G. de Graft, W. L. Driessen, J. Reedijk, J. P. Zanello, *J. Chem. Soc., Dalton Trans.* **1990**, 3175; R. Bastida, S. Gongalez, T. Rodríguez, A. Sousa, D. E. Fenton, *J. Chem. Soc., Dalton Trans.* **1990**, 3643; M. R. Malachonsk, M. Adams, N. Elia, A. L. Rheingold, R. S. Kelly, *J. Chem. Soc., Dalton Trans.* **1999**, 2177; L. Casella, M. Gullotti, R. Vigato, *Inorg. Chim. Acta* **1986**, *124*, 121; R. A. Allred, S. A. Hufner, K. Rudzka, A. M. Arif, L. M. Berreau, *Dalton Trans.* **2007**, 351–357.
- [2] M. E. Hossain, M. N. Alam, M. A. Ali, M. Nazimuddin, E. F. Smith, R. C. Hynes, *Polyhedron* **1996**, *15*, 973.
- [3] M. Matzapetakis, D. Ghosh, T. C. Weng, J. E. Penner-Hahn, V. L. Pecoraro, *Biol. Inorg. Chem.* **2006**, *11*, 876–890; M. Oue, A. Ishigahi, K. Kimura, Y. Matsue, T. Shono, *J. PolySci. Polym. Chem.* **1985**, *23*, 2033; T. K. Ronson, H. Adams, L. P. Harding, R. W. Harrington, W. Clegg, M. D. Ward, *Polyhedron* **2007**, *26*, 2000.
- [4] E. I. Solomon, R. K. Szilagy, S. D. George, L. Basumallick, *Chem. Rev.* **2004**, *104*, 419–458; D. B. Rorabacher, *Chem. Rev.* **2004**, *104*, 651; H. W. Yim, L. M. Tran, E. D. Dobbin, D. Rabinovich, L. M. Liablesands, C. D. Incarvito, K.-C. Larn, A. L. Rheingold, *Inorg. Chem.* **1999**, *38*, 2211–2215; P. Ge, B. S. Haggerty, A. L. Rheingold, C. G. Riordan, *J. Am. Chem. Soc.* **1994**, *116*, 8406–8407; A. J. Barton, J. Conolly, W. Levason, A. Mendia-Jalon, S. D. Orchard, G. Reid, *Polyhedron* **2000**, *19*, 1373–1379; P. L. Holland, W. B. Tolman, *J. Am. Chem. Soc.* **2000**, *122*, 6331–6332; J. A. Graden, M. C. Posewitz, J. R. Simon, G. N. George, I. J. Pickering, D. R. Winge, *Biochemistry* **1996**, *35*, 14583–14589.
- [5] I. Bertini, H. B. Gray, S. J. Lippard, J. S. Valentine, *Bioinorganic Chemistry*, University Science Books, Mill Valley, CA, **1994**; W. Kaim, B. Schwederski, *Bioinorganic Chemistry: Inorganic Elements in the Chemistry of Life*, J. Wiley & Sons, Chichester-New York-Brisbane-Toronto-Singapore, **1994**, pp. 22 and 196; P. M. Bush, J. P. Whitehead, C. C. Pink, E. C. Gramm, J. L. Eglin, S. P. Watton, L. E. Pence, *Inorg. Chem.* **2001**, *40*, 1871 and references cited therein.
- [6] T. Shi, J. Berglund, L. I. Elding, *Inorg. Chem.* **1996**, *35*, 3498; S. Choi, S. Mahalingaiah, S. Delaney, N. R. Neale, S. Massod, *Inorg. Chem.* **1999**, *38*, 1800; M. D. Hall, T. W. Hambley, *Coord. Chem. Rev.* **2002**, *232*, 49; E. Bouwman, W. L. Driessen, J. Reedijk, *Coord. Chem. Rev.* **1990**, *104*, 143.
- [7] R. Balamurugan, M. Palaniandavar, S. R. Gopalan, G. U. Kulkarni, *Inorg. Chim. Acta* **2004**, *357*, 919–930; M. Vidyathanan, R. Balamurugan, S. Usha, M. Palaniandavar, *J. Chem. Soc., Dalton Trans.* **2001**, 3498 and references cited therein.
- [8] B. C. Westerby, K. L. Juntunen, G. H. Leggett, V. B. Pett, M. J. Koenigbauer, M. D. Purgett, M. J. Taschner, L. A. Ochrymowycz, D. B. Rorabacher, *Inorg. Chem.* **1991**, *30*, 2109; K. K. Nanda, A. W. Addison, R. J. Butcher, M. R. McDevitt, T. N. Rao, E. Sinn, *Inorg. Chem.* **1997**, *36*, 134–135.
- [9] E. A. Ambundo, L. A. Ochrymowycz, D. B. Rorabacher, *Inorg. Chem.* **2001**, *40*, 5133–5138; L. Q. Hatcher, D.-H. Lee, M. A. Vance, A. E. Milligan, R. Sarangi, K. O. Hodgson, B. Hedman, E. I. Solomon, K. D. Karlin, *Inorg. Chem.* **2006**, *45*, 10055–10057.
- [10] U. S. Ray, B. Banerjee, G. Mostafa, T.-H. Lu, C. Sinha, *New J. Chem.* **2004**, *28*, 1432 and references cited therein.
- [11] T. K. Misra, D. Das, C. Sinha, *Polyhedron* **1997**, *16*, 4163.
- [12] J. Dinda, U. S. Ray, G. Mostafa, T.-H. Lu, A. Usman, I. A. Razak, S. Chantrapomma, H.-K. Fun, C. Sinha, *Polyhedron* **2003**, *22*, 247–255.
- [13] B. Banerjee, U. S. Ray, Sk. Jasimuddin, J.-C. Liou, T.-H. Lu, C. Sinha, *Polyhedron* **2006**, *25*, 1299–1306.
- [14] S. S. Tandon, L. K. Thompson, M. E. Manuel, J. N. Bridson, *Inorg. Chem.* **1994**, *33*, 5555; G. A. Albada, M. T. Lakin, N. Veldman, A. L. Spek, J. Reedijk, *Inorg. Chem.* **1995**, *34*, 4910; B. Graham, M. T. W. Hearn, P. C. Junk, C. M. Kepert, F. E. Mabbs, B. Moubaraki, K. S. Murray, L. Spiccia, *Inorg. Chem.*

- 2001, 40, 1536; P. Manikandan, R. Muthukumar, K. R. J. Thomas, B. Varghese, G. V. R. Chandramouli, P. T. Manoharan, *Inorg. Chem.* **2001**, 40, 2378; S. Koner, S. Saha, T. Malah, K.-I. Okamoto, *Inorg. Chem.* **2004**, 43, 840; J. D. Woodward, R. V. Backov, K. A. Abboud, D. Dai, H.-J. Koo, M.-H. Whangbo, M. W. Meisel, D. R. Talham, *Inorg. Chem.* **2005**, 44, 638; Y.-F. Zeng, X. Hu, F.-C. Liu, X.-H. Bu, *Chem. Soc. Rev.* **2009**, 38, 469; A. Escuer, G. Aromí, *Eur. J. Inorg. Chem.* **2006**, 4721.
- [15] D. A. Buckingham, *Coord. Chem. Rev.* **1994**, 587, 135; A. Escuer, M. A. S. Goher, F. A. Mautner, R. Vicente, *Inorg. Chem.* **2000**, 39, 2107; M. A. S. Goher, A. Escuer, F. A. Mautner, N. A. Al-Salem, *Polyhedron* **2001**, 20, 2971; S. Koner, S. Saha, K.-I. Okamoto, J. P. Tuchagues, *Inorg. Chem.* **2003**, 42, 4668.
- [16] U. S. Ray, Sk. Jasimuddin, B. K. Ghosh, M. Monfort, J. Ribas, G. Mostafa, T.-H. Lu, C. Sinha, *Eur. J. Inorg. Chem.* **2004**, 250; U. S. Ray, K. K. Sarker, G. Mostafa, T.-H. Lu, Md. S. El Fallah, C. Sinha, *Polyhedron* **2006**, 25, 2764.
- [17] D. A. Robb in *Copper Proteins and Copper Enzymes* (Ed.: R. Lontie), CRC Press, Inc., Boca Raton, Florida, **1984**, vol. 2, pp. 207; K. D. Karlin, Z. Tyeklar, *Bioinorganic Chemistry of Copper*, Chapman & Hall, New York, **1993**; W. Kaim, B. Schwederski, *Bioinorganic Chemistry: Inorganic Elements in the Chemistry of Life*, J. Wiley & Sons, Chichester-New York-Brisbane-Toronto-Singapore, **1994**, pp. 22 and 196; K. Krylova, C. P. Kulatilike, M. J. Heeg, C. A. Salhi, L. A. Ochrymowycz, D. B. Rorabacher, *Inorg. Chem.* **1999**, 38, 4322.
- [18] D. Das. Ph. D. Thesis, **1998**, Burdwan University, Burdwan, 713 104, India; P. Bhunia, B. Baruri, U. S. Ray, C. Sinha, S. Das, J. Cheng, T.-H. Lu, *Transition Met. Chem.* **2006**, 31, 310–315; J. Otsuki, K. Suwa, K. Narutaki, C. Sinha, I. Yoshikawa, K. Araki, *J. Phys. Chem. A* **2005**, 109, 8064–8069.
- [19] D. Datta, A. Chakravorty, *Inorg. Chem.* **1983**, 22, 1085.
- [20] V. Kalsani, M. Schmittel, A. Listori, G. Accorsi, N. Armaroli, *Inorg. Chem.* **2006**, 45, 2061–2067.
- [21] O. Kahn, S. Sikarov, J. Gouteron, S. Jeannin, *Inorg. Chem.* **1983**, 22, 2877.
- [22] P. K. Dhara, S. Pramanik, T.-H. Lu, M. G. B. Drew, P. Chattopadhyay, *Polyhedron* **2004**, 23, 2457.
- [23] S. Torelli, C. Belle, C. Philouze, J.-L. Pierre, W. Rammal, E. Saint-Aman, *Eur. J. Inorg. Chem.* **2003**, 2452–2457; B. Adhikari, C. R. Lucas, *Inorg. Chem.* **1994**, 33, 1376.
- [24] A. B. P. Lever, *Inorganic Electronic Spectroscopy*, Elsevier, Amsterdam, **1984**.
- [25] B. Bleaney, K. D. Bowers, *Proc. Roy. Soc. (London) Ser. A* **1952**, 214, 451.
- [26] O. Kahn, *Molecular Magnetism*, VCH Publishers, New York, **1993**.
- [27] R. Boca, *Struct. Bonding (Berlin)* **2006**, 117, 1 and references cited therein.
- [28] The series of calculations were made with the computer program CLUMAG, which uses the irreducible tensor operator (ITO) formalism: D. Gatteschi, L. Pardi, *Gazz. Chim. Ital.* **1993**, 123, 231.
- [29] J. Ribas, A. Escuer, M. Monfort, R. Vicente, R. Cortés, L. Lezama, T. Rojo, *Coord. Chem. Rev.* **1999**, 193–195, 1027 and references cited therein.
- [30] E. Ruiz, J. Cano, S. Alvarez, P. Alemany, *J. Am. Chem. Soc.* **1998**, 120, 11122 and references cited therein.
- [31] S. S. Tandon, L. K. Thompson, M. E. Manuel, J. N. Bridson, *Inorg. Chem.* **1994**, 33, 5555.
- [32] P. J. Hay, J. C. Thibeault, R. Hoffmann, *J. Am. Chem. Soc.* **1975**, 97, 4884.
- [33] B. K. Santra, P. A. N. Reddy, A. Chakravarty, *Inorg. Chem.* **2002**, 41, 1328.
- [34] A. I. Vogel, *A Text Book of Practical Organic Chemistry*, 2nd ed., Longman, London, **1959**.
- [35] G. M. Sheldrick, *SHELXTL, Crystallographic Software Package, Version 6.10*, Bruker-AXS, Madison, WI, **2002**; G. M. Sheldrick, *SHELXL 97, Program for the Refinement of Crystal Structure*, University of Göttingen, Germany, **1997**.
- [36] G. M. Sheldrick, *SHELXS-97, Program for the Solution of Crystal Structure*, University of Göttingen, Germany, **1997**.
- [37] ORTEP-3 for Windows, L. J. Farrugia, *J. Appl. Crystallogr.* **1997**, 30, 565.
- [38] A. L. Spek, *PLATON, Molecular Geometry Program*, University of Utrecht, The Netherlands, **1999**.
- [39] M. J. Frisch, G. W. Trucks, H. B. Schlegel, P. M. W. Gill, B. G. Johnson, M. A. Robb, J. R. Cheeseman, T. A. Keith, G. A. Petersson, J. A. Montgomery, K. Raghavachari, M. A. Al-Laham, V. G. Zakrzewski, J. V. Ortiz, J. B. Foresman, J. Cioslowski, B. B. Stefanov, A. Nanayakkara, M. Challacombe, C. Y. Peng, P. Y. Ayala, W. Chen, M. W. Wong, J. L. Andres, E. S. Replogle, R. Gomperts, R. L. Martin, D. J. Fox, J. S. Binkley, D. J. Defrees, J. Baker, J. P. Stewart, M. Head-Gordon, C. Gonzalez, J. A. Pople, *Gaussian98*, Gaussian, Inc., PA Pittsburgh, **1998**.
- [40] C. Lee, W. Yang, R. G. Parr, *Phys. Rev. B* **1988**, 37, 785–789.
- [41] P. J. Hay, W. R. Wadt, *J. Chem. Phys.* **1985**, 82, 270.
- [42] M. Cossi, V. J. Barone, *J. Chem. Phys.* **2001**, 115, 4708.

Received: July 10, 2009

Published Online: November 24, 2009